Proc. Estonian Acad. Sci. Eng., 2001, **7**, 4, 309–330

ON FREQUENCY ADAPTATION IN AN EXTENDED BLOCK-ADAPTIVE FOURIER ANALYSER

Ants RONK

Department of Electronics, Tallinn Technical University, Ehitajate tee 5, 19086 Tallinn, Estonia; ronk@ttu.ee

Received 2 May 2001, in revised form 2 October 2001

Abstract. The aim of this work is to form a basis for developing an efficient adaptive multi-frequency adaptation algorithm for an extended block-adaptive Fourier analyser (EBAFA), which performs simultaneously separation and analysis of its input signal's periodic components of different frequencies and waveforms. A brief description of EBAFA is given and several possibilities to improve estimation of differences between fundamental frequencies of signal's periodic components and corresponding resonator groups of EBAFA are considered.

Key words: adaptive filters, observers, resonators, spectral analysis, waveform analysis, frequency estimation.

1. INTRODUCTION

In several experiments the measurement signal contains non-harmonic periodic components of different frequencies and waveforms. Often such components carry information about different processes and one should analyse them separately, sometimes in real time. Besides, these components can be non-stationary (of varying frequency and harmonic content) and a noise may be added to them (as it is, for example, in a hand-to-hand bio-impedance signal containing heartbeat and breathing components [1]). Traditional filtering is not suited for solving such tasks but adaptive filtering is often applicable [2], if one can use additional information (for example, in the form of a reference signal) that permits suppression of the signal's undesired components. On the other hand, phase-locked loop based systems [3] can be used to separate the 1st and also higher harmonics of the useful component from the composite measurement signal, if the fundamental frequency of this component is known precisely enough.

In [4], an alternative to the above was proposed in the form of an extended block-adaptive Fourier analyser (EBAFA). It was developed mostly on the basis of works by Hostetter, Péceli, Nagy and Simon [5–8], devoted to the algorithms for recursive discrete Fourier transform that can be considered as observers [9]. EBAFA is a tool for processing band-limited discrete-time signals $x(k)$ that can be presented in the form

$$x(k) = \sum_{q=0}^{Q} x_q(k), \tag{1}$$

where k is the number of the sampling step, $x_0(k) = A_{0,0}$ is a constant, and

$$x_q(k) = \sum_{\substack{n=-N_q \\ n\neq 0}}^{N_q} A_{q,n}\, e^{j\omega_q nk}, \quad q = 1,\ 2,\ ...,\ Q \tag{2}$$

are periodic components. In Eq. (2) $A_{q,n}$ is the nth complex Fourier coefficient of the signal's qth component, which has a fundamental frequency ω_q and the number of the highest harmonic N_q. It is assumed that $N_q\omega_q$ is smaller than the Nyquist frequency.

EBAFA makes it possible to separate signal's periodic components and to find their spectra simultaneously in real time (of course, several restrictions exist; for example, sufficiently precise initial estimates of the components' fundamental frequencies must be used, etc.). However, as stated in [4], EBAFA should be improved for wider practical application. This paper is focused on finding and analysing ways to develop for EBAFA an efficient adaptive algorithm for multi-frequency adaptation.

2. THEORETICAL BASIS

EBAFA of the order Q (its block diagram is presented in Fig. 1) enables us to find estimates of the constant component and Q real periodic components of its input signal $x(k)$ as $\hat{x}_q(k)$, estimates $\hat{\omega}_q$ of corresponding fundamental frequencies ω_q, and also estimates of complex Fourier coefficients of the periodic components $X_m(k)$, $m = \pm 1, \pm 2, ..., \pm L$. If $Q = 1$, EBAFA turns into a simple block-adaptive Fourier analyser (BAFA) [8], where $\hat{x}_0(k)$ (the estimate of the constant component $x_0(k)$) is determined as $X_0(k)$ (as an estimate of the 0th Fourier coefficient of $x(k) = x_1(k)$). Thus in the following we consider basic properties of the BAFA, because they match with those of the EBAFA, which are essential for us.

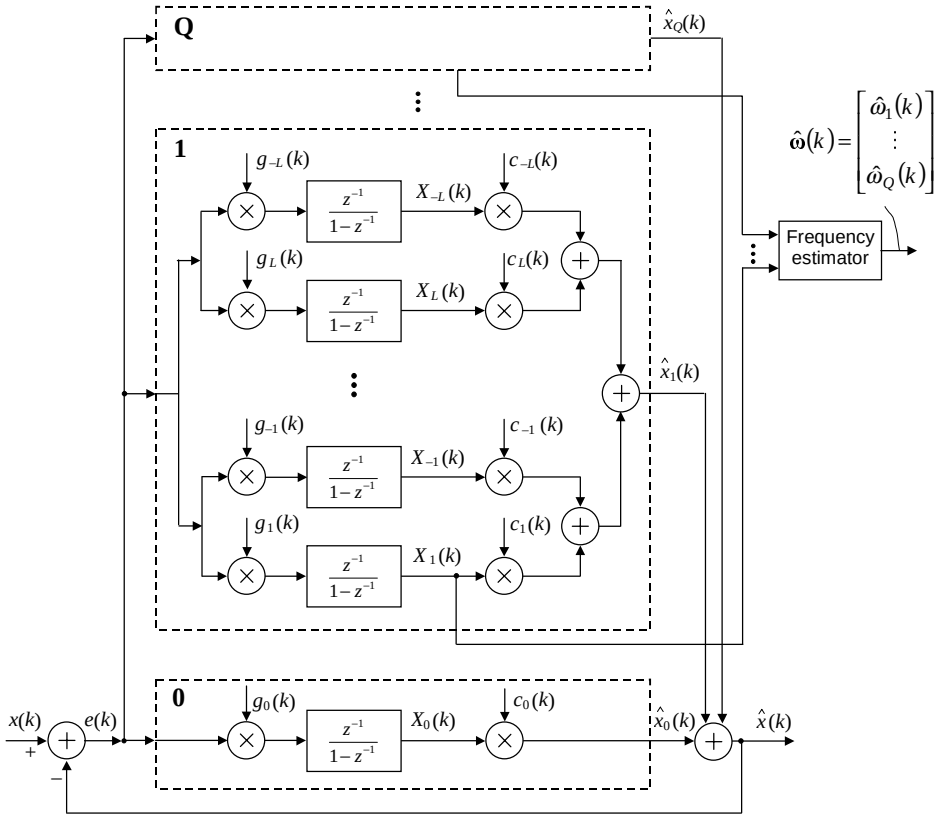

Fig. 1. Block diagram of an extended block-adaptive Fourier analyser (EBAFA) of the order Q (in case of $Q=1$ one obtains a BAFA).

2.1. Basics of the BAFA

BAFA consists of $M=2L+1$ harmonically related parallel resonators (EBAFA's resonator groups **0** and **1** in Fig. 1) with a common negative feedback. The number of resonator pairs in BAFA (the number of formed harmonics L) depends on the fundamental frequency $\hat{\omega}_1$ of the BAFA's resonators and it must satisfy the inequality

$$\pi/\hat{\omega}_1 - 1 \le L < \pi/\hat{\omega}_1. \tag{3}$$

In BAFA, the variable coefficients $c_m(k)$ and $g_m(k)$ of the resonators in Fig. 1 are computed as follows:

$$c_m(k) = e^{j\hat{\omega}_1 mk}, \tag{4}$$

$$g_m(k) = r_m\, e^{-j\hat{\omega}_1 mk} = r_m / c_m(k), \tag{5}$$

where the coefficients

$$r_m = \prod_{\substack{i=-L \\ i\neq m}}^{L} \left(1 - z_i\, z_m^{-1}\right)^{-1}, \quad z_i = e^{j\hat{\omega}_1 i} \tag{6}$$

are such that the system has poles only at the origin and operates as a dead-beat observer with transient length equal to the total number of resonators M (for the EBAFA of the order $Q > 1$, expressions (5) and (6) are more complicated [4]).

Let us assume that a signal (1) with $Q = 1$ is processed in BAFA.

If $\hat{\omega}_1 = \omega_1$ (the fundamental frequencies of the resonator system and of the input signal have been set equal) and also $L = N_1$, then, after passing M sampling intervals, the desired result $X_m(k) = A_{1,m}$ is obtained for $m = -L, ..., -1, 0, 1, ..., L$.

If $\hat{\omega}_1 \neq \omega_1$, then the Fourier coefficients' estimates $X_m(k)$ (the state variables of BAFA, which is a spectral observer) are erroneous; for example, the 1st Fourier coefficient has the form

$$X_1(k) = \sum_{m=-L}^{L} X_{1,m}(k) = \sum_{m=-L}^{L} \tilde{A}_m e^{j(\omega_1 m - \hat{\omega}_1)k}, \tag{7}$$

where

$$\tilde{A}_m = A_{1,m} T_1(e^{j\omega_1 m}), \tag{8}$$

and the transfer function of the mth channel from the input $x(k)$ to $X_m(k)\, c_m(k)$ is

$$T_m(z) = \frac{r_m z_m z^{-1}}{1 - z_m z^{-1}} \left(1 + \sum_{i=-L}^{L} \frac{r_i z_i z^{-1}}{1 - z_i z^{-1}}\right)^{-1}, \quad z_i = e^{j\hat{\omega}_1 i}. \tag{9}$$

The unwrapped angle between the complex vectors $X_{1,1}(l+P)$ and $X_{1,1}(l)$ can be expressed as

$$\Phi_{1,1}(l+P, l) = \angle\left(X_{1,1}(l+P) \big/ X_{1,1}(l)\right) = P(\omega_1 - \hat{\omega}_1). \tag{10}$$

This opens the possibility to estimate the frequency error $\Delta\omega_1 = \omega_1 - \hat{\omega}_1$ and to update further $\hat{\omega}_1$ and the parameters of BAFA according to Eqs. (3)–(6). The whole procedure of the frequency error estimation should be performed only when the transients (caused by the previous parameter updating or by changes in the input signal) have decayed, otherwise an additional estimation error appears.

2.2. Frequency error estimation in BAFA

Assuming that the stationary input signal is such that in BAFA for all $m \neq 1$, $\tilde{A}_m << \tilde{A}_1$ in Eq. (7), the frequency error estimate $\Delta\hat{\omega}_1$ can be found as

$$\Delta\hat{\omega}_1 = \frac{\Phi_1(l+P,l)}{P} = \frac{\angle(X_1(l+P)/X_1(l))}{P}, \tag{11}$$

where $\Phi_1(l+P,l)$ is the angle between the vectors presenting the complex valued estimates of the 1st Fourier coefficient computed in sampling steps $l+P$ and l. The unwrapped angle $\Phi_1(l+P,l)$ between two vectors can be computed, assuming

$$\left|\Phi_1(l+P,l)\right| < \pi. \tag{12}$$

In [7], angle measurements in Eq. (11) were performed in every time-step using $P=1$, but in [8] block-adaptation was applied (with the aim to perform convergence analysis of BAFA) using $P>1$ and performing frequency error estimation only after the transients had decayed. In case of $P=2L$, practically the same frequency convergence speed was achieved as in [7].

As stated in [8], the frequency convergence can be achieved, if relative amplitudes of the input signal's Fourier components satisfy the inequality

$$a_n \geq \left|A_n\right| / \left|A_1\right|. \tag{13}$$

In order to relax these restrictions and to improve precision of the frequency error estimation, we propose to condition the vectors used in angle measurement (Eq. (11)). The conditioning means processing of the computed values $X_1(i)$ according to an algorithm $\boldsymbol{\tau}$, which finds for pairs of properly chosen sets of computed values $X_1(i)$, shifted in time by P, corresponding pairs of such complex vectors $X_{\tau,P}$ and $X_{\tau,0}$ that the angle $\Phi_{\tau,P}$ between them is closer to $\Phi_{1,1}(l+P,l)$ (Eq. (10)) than $\Phi_1(l+P,l)$ in Eq. (11), and permits thus to obtain a better estimate of the error

$$\Delta\hat{\omega}_1 = \frac{\Phi_{\tau,P}}{P} = \frac{\angle(X_{\tau,P}/X_{\tau,0})}{P}. \tag{14}$$

The latter corresponds to the unwrapped angle

$$\left|\Phi_{\tau,P}\right| < \pi. \tag{15}$$

2.3. Vector conditioning for angle measurement

In [10] it was proposed to use for conditioning an algorithm that forms $X_{\tau,P}$ and $X_{\tau,0}$ as average values of B consecutive complex vectors (values of the 1st Fourier coefficients) chosen with the time-shift P:

$$X_{\tau,p} = \frac{1}{B}\sum_{i=0}^{B-1} X_1(l+p+i), \quad p = 0, P. \tag{16}$$

The vector diagram in Fig. 2 demonstrates how this algorithm leads to the desired result (details are given in [10]).

It has been shown also that, if Eq. (16) is used to find $X_{\tau,0}$ and $X_{\tau,P}$, then the upper limit Ψ for the angle error $\left|\Phi_{1,1}(l+P,l) - \Phi_{\tau,P}\right|$, which is proportional to the error of the frequency error estimate (14), can be expressed in the form

$$\Psi = 2\arcsin \sum_{\substack{m=-L \\ m\neq 1}}^{L} \frac{\left|\tilde{A}_m\right|}{\left|\tilde{A}_1\right|}\gamma_m \geq \left|\Phi_{1,1}(l+P,l) - \Phi_{\tau,P}\right|, \tag{17}$$

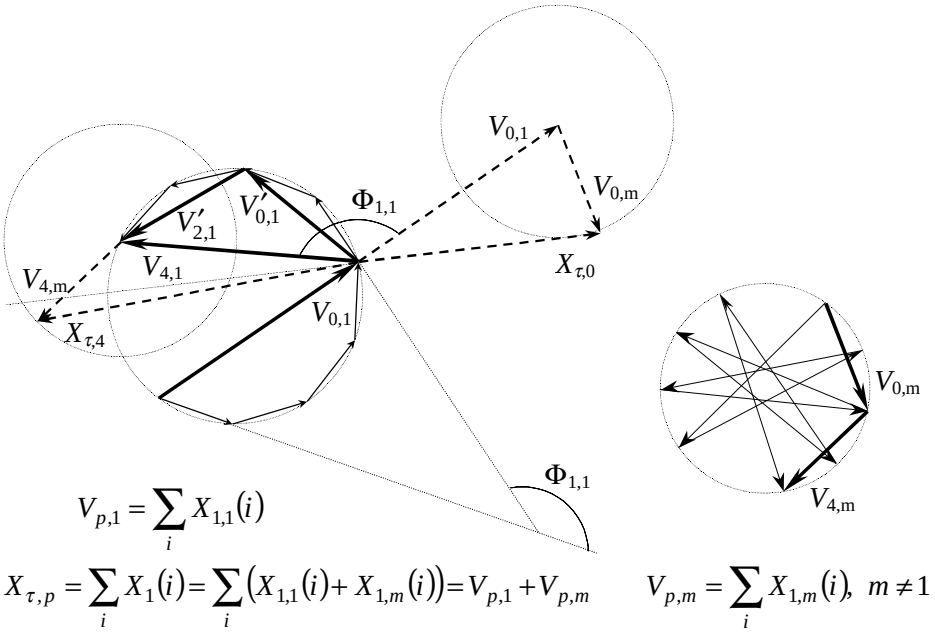

Fig. 2. Vector diagram of conditioning the vector $X_1(i) = X_{1,1}(i) + X_{1,m}(i)$ applying Eq. (16).

where

$$\gamma_m = \left| \frac{\sin \dfrac{\hat{\omega}_1 \delta_1}{2(1-\delta_1)}}{\sin \dfrac{B\hat{\omega}_1 \delta_1}{2(1-\delta_1)} \sin \dfrac{\hat{\omega}_1 (m-1+\delta_1)}{2(1-\delta_1)}} \right| \tag{18}$$

is a relative disturbance gain, introduced by vector conditioning with $B>1$ (in [8], $\gamma_m \equiv 1$ was obtained for the case $B=1$), and

$$\delta_1 = \Delta\omega_1/\omega_1 = (\omega_1 - \hat{\omega}_1)/\omega_1 . \tag{19}$$

It was shown also that increasing of B permits us to increase the precision of $\Delta\hat{\omega}_1$ in Eq. (14) only if

$$B < \pi/\Delta\omega_1 , \quad \text{or} \quad B \le L\left|\delta_1^{-1} - 1\right| < \pi/\Delta\omega_1 . \tag{20}$$

One can easily find that the frequency error estimation with such vector conditioning is nearly time-optimal, if $B \approx P$. In this case Eq. (20) is not needed and only the inequality (15) must be satisfied to ensure acceptability of values of the parameters P and $B \approx P$. Besides, if $\delta_1 \to 0$ and $P, B \to L\left|\delta_1^{-1} - 1\right| \to \infty$, the error of the frequency error estimate is $\Omega(P^{-2})$ instead of $\Omega(P^{-1})$ for the basic estimator [8].

It is evident that vector conditioning can be performed in several ways, for example, by adding vectors $X_1(i)$ separately for odd and even steps:

$$X_{\tau,p} = \frac{1}{B}\sum_{i=0}^{B-1} X_1(l + p + 2i), \quad p = 0,\ 1, \tag{21}$$

where B must satisfy (20). Here $P=1$, because the angle between the resultant vectors is an estimate of the frequency error $\Delta\omega_1$. The corresponding algorithm may be useful for suppressing errors caused by input signal's components of frequencies, which are close to ω_1. One does not need it in the BAFA, but it may be important for the EBAFA.

The above approaches can be realized by an algorithm $\tau(P, B)$, which gives

$$X_{\tau(P,B),p} = \frac{1}{B}\sum_{k=0}^{D-1}\sum_{i=2Pk}^{2Pk+P-1} X_1(l + p + i), \quad p = 0, P,$$
$$B = DP, \quad 2B - P = (2D-1)P < \pi/\Delta\omega_1. \tag{22}$$

It is possible that in some cases the resultant vectors should be found using a more general and more powerful, but also more time-consuming algorithm $\tau_\infty(P, B)$, which permits processing of larger sets of vectors:

$$X_{\tau_\infty(P,B),p} = \frac{1}{B}\sum_{b=1}^{b_\infty}\sum_{k=S_{b-1}}^{S_b-1}\sum_{i=2Pk}^{2Pk+P-1} X_1(l+p+i)\,(-1)^b, \quad p=0,P,$$

$$S_b = S_{b-1} + D_b, \qquad S_0 = 0, \qquad P(2D_b - 1) \approx \pi/\Delta\omega_1,$$

$$B = P\sum_{b=1}^{b_\infty} D_b, \qquad 2B - b_\infty P = P\sum_{b=1}^{b_\infty}(2D_b - 1) \approx b_\infty \pi/\Delta\omega_1, \tag{23}$$

or realizes an analogous but simpler extension of (16):

$$X_{\tau_\infty(P,B),p} = \frac{1}{B}\sum_{b=1}^{b_\infty}\sum_{i=S_{b-1}}^{S_b-1} X_1(l+p+i)\,(-1)^b, \quad p=0,P,$$

$$S_b = S_{b-1} + D_b, \quad S_0 = 0, \quad D_b \approx \pi/\Delta\omega_1, \quad B = \sum_{b=1}^{b_\infty} D_b \approx b_\infty \pi/\Delta\omega_1. \tag{23a}$$

Efficiency of the proposed more general algorithms depends on the content of the (E)BAFA's input signal (frequencies of its periodic components, amplitudes of harmonics) and on the choice of the values of P (which has to keep the inequality (15) satisfied) and B (that is, D or b_∞, and D_b). Values of these parameters can be chosen in the computation process depending on the obtained results, and this enables us to develop an adaptive frequency error estimator.

The above vector conditioning algorithms offer a possibility to improve frequency error estimation without enlarging the set of saved samples (needed memory) via performing joint vector conditioning and angle enlargement.

2.4. Angle enlargement for frequency error estimation

Let us consider a vector diagram of vector conditioning according to Eq. (16) with $B = P$, presented in Fig. 2. When the vector conditioning process has ended (according to the inequality (15)) and angle measurement performed using $X_{\tau,4}$ and $X_{\tau,0}$, then, if only P latest samples $X_1(i)$ are held in the memory, a new conditioning/measurement cycle can be performed, for example, according to one of the following two schemes.

Scheme 1. One can compute new vectors $X'_{\tau,2}$ and $X'_{\tau,0}$ on the basis of values of the components of $X_{\tau,4}$ (that is, $X_1(i)$), which are in the memory at this moment, and further update them (using new samples of $X_1(i)$) until the next final $X'_{\tau,P}$ and $X'_{\tau,0}$ are fixed due to the unsatisfied inequality (15) (it may happen that $B = P \neq 4$ in this measurement cycle!). Figure 2 illustrates the start

of this cycle and shows how $V'_{2,1}$ and $V'_{0,1}$ (the useful components of $X'_{\tau,2}$ and $X'_{\tau,0}$) are obtained summing $X_{1,1}(i)$ (useful components of $X_1(i)$). In the experiments, the results of which are given in Section 3, we apply only this scheme.

Scheme 2. In certain conditions, for example, when in the case shown in Fig. 2 achievement of $B = P = 4$ is guaranteed in the following angle measurement cycles, one can set $X'_{\tau,0} = X_{\tau,4}$ and find $X_{\tau,4}$ using new samples of $X_1(i)$.

After performing M_c angle measurement cycles, the frequency error estimate can be computed as

$$\Delta\hat{\omega}_1 = \frac{\Phi_{\tau,P_\Sigma}}{P_\Sigma} = \frac{\sum_{m=1}^{M_c} \Phi_{\tau,P_m}}{\sum_{m=1}^{M_c} P_m}. \tag{24}$$

Consequently, using in Eq. (14) instead of $\Phi_{\tau,P}$ and P the sums of corresponding results of the measurement cycles, we obtain $\Phi_{\tau,P_\Sigma} = \sum_m \Phi_{\tau,P_m}$, which is a practically unlimited unwrapped angle, and $P_\Sigma = \sum_m P_m$, both found over the set of performed cycles.

In the scheme 2 the error's limit (17) remains valid for the total angle Φ_{τ,P_Σ} due to the fact that $P_m = P_1 = P$ and $X_{\tau,0\,m} = X_{\tau,P_{m-1}}$ for $m = 2,3,...,M_c$. Then it is possible to choose (at the end of the first angle measurement cycle) such a number M_c of the angle measurement cycles that the upper limit of the absolute relative worst-case error of the frequency error estimate (24), which can be expressed as

$$\delta_{\lim}(\Delta\hat{\omega}_1) = \Psi \Big/ \left| \sum_{m=1}^{M_c} \Phi_{\tau,P_m} \right| \approx \Psi \Big/ \left(M_c \left| \Phi_{\tau,P_1} \right| \right), \tag{25}$$

becomes sufficiently small.

Assumption $P_m = P_1 = P$ for $m = 2,3,...,M_c$ means that P must satisfy, instead of (15), the inequality

$$\left| \Phi_{\tau,P}(k) \right| < \pi - 2\psi, \tag{26}$$

where ψ is such estimate of the unknown angle error's limit Ψ that $\pi > \psi > \Psi$. Of course, ψ should be minimal.

If up to $2P$ latest values of $X_1(i)$ are held in the memory in the vector conditioning process, then after finding the vectors $X_{\tau,P}(k)$ and $X_{\tau,0}(k)$ and the frequency error estimate (14) in the time-step k, one can easily find corresponding vectors in following time-steps, but only if (15) remains satisfied in case of increasing k (if (26) holds for the first value of k). One can also find (over the set of computed $X_{\tau,p}(l)$)

$$X_{\tau,\max} = \max_{p,l} \left| X_{\tau,p}(l) \right| \quad \text{and} \quad X_{\tau,\min} = \min_{p,l} \left| X_{\tau,p}(l) \right|, \tag{27}$$

which can be used to compute

$$\hat{\Psi} = 2 \arcsin \frac{X_{\tau,\max} - X_{\tau,\min}}{X_{\tau,\max} + X_{\tau,\min}}. \tag{28}$$

In certain favourable conditions $\hat{\Psi}$ can be considered as an approximate (but, unfortunately, underestimated) value of the angle error's upper limit Ψ. Then, if ψ permits one to find $\Delta\hat{\omega}_1$ and $\hat{\Psi}$ according to Eqs. (24) and (28), one can update $\hat{\omega}_1$ and (with special precaution) also ψ. On the other hand, a significant increase of currently computed (small) values of $\hat{\Psi}$ indicates essential changes in the input signal. If $X_{\tau,\max} = \max_l |X_1(l)|$ and $X_{\tau,\min} = \min_l |X_1(l)|$ are used in (28), then the value $\hat{\Psi}$ is obtained for Ψ, which corresponds to $\gamma_m \equiv 1$.

2.5. Frequency error estimation and frequency updating in EBAFA

In EBAFA the frequency error estimators of all the resonator groups can start to work simultaneously after the transients have decayed. As our experiments have shown, it is reasonable (in the sense of total transient time or multi-frequency convergence speed) to update fundamental frequencies (and frequency-dependent parameters) of all the resonator groups in the same time-step. Thus, the work of the frequency error estimators must be organized to achieve:

1) optimal (or at least reasonable) estimation time,
2) efficient using of this time in all the estimators.

Due to the large amount of different factors (frequencies, phases and spectra of the input signal components, noise, disturbances) that have influence on the processes in EBAFA, it is difficult to find an optimal solution for this task. It seems to be reasonable to make EBAFA adaptive enough to more essential factors and stable in critical situations.

Let us consider here some features of the EBAFA's last versions, used in the experiments, the results of which are presented in Section 3.

1. Coefficients K_q were introduced to determine numbers of time-steps for frequency error estimation (that is, $2B$ for Eqs. (21) to (23), and its equivalent $B+P$ for Eqs. (16) and (23a)) for all resonator groups from the equation

$$2B_q = K_q L_q, \quad q = 1, 2, ..., Q. \tag{29}$$

The values of the coefficients K_q were computed as

$$K_q = \left[0.5 + K\hat{\omega}_q \Big/ \min_q \{\hat{\omega}_q\} \right], \tag{30}$$

where K is a common parameter for determining the estimation time. Later the formula

$$2B_q = \left[K\pi \Big/ \min_q \{\hat{\omega}_q\} \right] \tag{31}$$

was used.

2. When all Q frequency error estimates have been found, only these new values of the EBAFA's fundamental frequencies, which lie in the pre-set working bands, that is, satisfy the inequalities

$$\hat{\omega}_{q,\min} < \hat{\omega}_q + \Delta\hat{\omega}_q < \hat{\omega}_{q,\max}, \tag{32}$$

are accepted and taken into use. The frequency limits $\hat{\omega}_{q,\min}$ and $\hat{\omega}_{q,\max}$ (and the initial value of $\hat{\omega}_q$) should be fixed using available information about ω_q, in accordance with other essential factors. It is expected that the restriction (32) excludes possible large errors in the first steps of the multi-frequency convergence process.

The above features permit investigation and control of signal processing in the EBAFA *en bloc* and they are closely related; for example, a greater K_q enables to obtain a better estimate $\Delta\hat{\omega}_q$ but it assumes a smaller initial error $\Delta\omega_q$ [10]. On the other hand, in case of $\omega_q > \omega_p$ one should use $K_q > K_p$ to achieve in the process of estimation of $\Delta\omega_q$ sufficient suppression of errors, caused by lower harmonics of the *p*th component, etc. In order to obtain some information for further studies, we performed several pilot experiments simulating the work of the EBAFA in the MATLAB environment.

3. SIMULATION RESULTS

In this section multi-frequency convergence processes and separation of the signal's components in the EBAFA are considered, but first some earlier results on frequency error estimation in the BAFA are presented.

3.1. A case study: BAFA's input signal is a sum of two (not harmonically related) sinusoids

It can be shown that if the BAFA's input signal consists of a useful sinusoid of a frequency $\omega_u = \omega_1$ with an amplitude $A_u = 1$, and a disturbing sinusoid of a frequency ω_d with an amplitude A_d, then the angle error limit (17) (that is proportional to the limit of the error of the frequency error estimate) can be computed as

$$\Psi = 2\arcsin(\gamma(-\omega_1) + \theta\gamma(\omega_d) + \theta\gamma(-\omega_d)), \tag{33}$$

where

$$\theta = A_d \left| T_1(e^{j\omega_d}) \right| \cdot \left| T_1(e^{j\omega_1}) \right|^{-1}, \tag{34}$$

and

$$\gamma(\omega) = \left| \frac{\sin \dfrac{\hat{\omega}_1 \delta_1}{2(1-\delta_1)}}{\sin \dfrac{B\hat{\omega}_1 \delta_1}{2(1-\delta_1)} \sin \dfrac{\omega - \hat{\omega}_1}{2}} \right|. \tag{35}$$

We computed Ψ according to (33), using $\hat{\omega}_1 = \pi \cdot 10^{-2}$. The value of ω_1 was determined via $\hat{\omega}_1$ and δ_1. The parameters ω_d and A_d had such values that satisfied the equalities $\omega_{d+}\omega_{d-} = \omega_1^2$ and $A_{d+}A_{d-} = 1$, and also the inequalities $10^{-2} \le A_d \le 10^2$ and $(L+1)^{-1} \le \overline{\omega}_d = \omega_d / \omega_1 \le L+1$. In order to compare the frequency error estimates with [8] and [10], different values of the parameter B were used. If $B = 1$, then the estimator proposed in [10] matches with that described in [8]. As Eq. (35) gives for a small B such γ that overestimates the angle error limit, we used in Eq. (33) $\gamma \equiv 1$ in case of $B = 1$ (further $B = 1^{\gamma}$ is used to notify that).

The angle error upper limit Ψ can be found only if the absolute value of the argument of arcsin(·) in Eq. (33) is less than 1, and $\Psi < \pi - |\omega_1 - \hat{\omega}_1|$. If in our computations the first condition was not satisfied, then Ψ was set equal to π. As $|\omega_1 - \hat{\omega}_1| = |\delta_1|\omega_1$ was rather small, the region of parameters, where $\Psi < \pi$, can be considered as a domain of the BAFA's potential convergence (to guarantee actual convergence, the condition $P > \Psi / |\omega_1 - \hat{\omega}_1|$ must be satisfied).

Let us consider some simulation results, plotted using logarithmic presentation.

Figure 3 demonstrates how the domain of the BAFA's potential convergence, which remains below zero level due to the normalization of Ψ by π, enlarges with increasing B. In the lower half of the plots one can see a part of the region, where a constant error level caused by $\delta_1 = 0.3$ (the 1st complex Fourier component of the useful sinusoid) is greater than the error caused by the disturbing sinusoid.

Figure 4 presents the ratios of the angle error limits Ψ for the estimates according to [8] and [10]. These plots show that the introduced vector conditioning suppresses the estimate errors (caused by a disturbing sinusoidal signal of frequency $\omega_d \neq \omega_1 \approx \hat{\omega}_1$) as a simple low-pass filter, which has a resonant peak at the corner frequency $\hat{\omega}_1$, an asymptotic slope -20 dB per decade at higher frequencies, and an asymptotic level of $20\log(2L/(\pi B))$ dB in the pass-band.

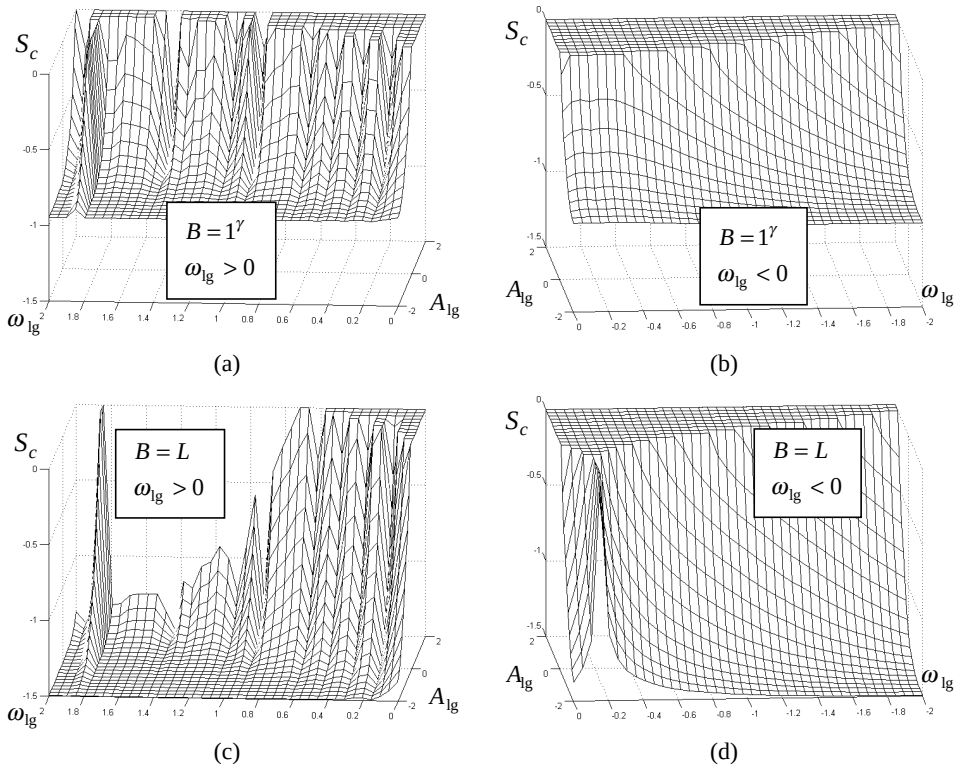

Fig. 3. Dependence of $S_c = \log(\Psi(\overline{\omega}_d, A_d, B)/\pi)$ on $\omega_{\lg} = \log(\overline{\omega}_d)$ and $A_{\lg} = \log(A_d)$ for two values of B; $\delta_1 = 0.3$.

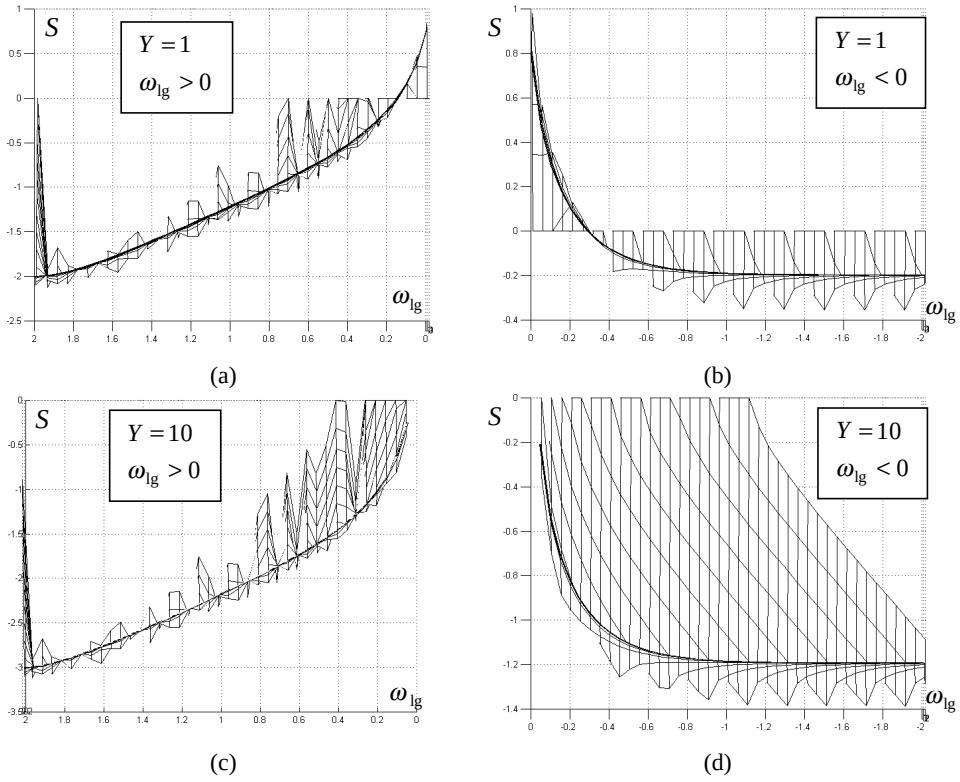

Fig. 4. Dependence of $S = \log(\Psi(\overline{\omega}_d, A_d, B = YL) \big/ \Psi(\overline{\omega}_d, A_d, B = 1^{\gamma}))$ on $\omega_{\lg} = \log \overline{\omega}_d$ and $A_{\lg} = \log A_d$ for different values of Y; the axis of $A_{\lg}$ is perpendicular to the surface of the plots; $\delta_1 = 10^{-10}$ (from [8,10]).

The ratios of the angle error limits Ψ (Fig. 5) have been found so that in case of $\Psi_1 < \Psi_2 = \pi$ the ratio Ψ_1 / Ψ_2 was set equal to 10^{-5}. The plotted surfaces give an approximate description of the worst-case possibilities to maintain frequency convergence in EBAFA, where the fundamental frequencies of its resonator groups that correspond to the input signal's sinusoidal components of frequencies ω_1 and ω_d, have the same error δ_1:

1) in a small horizontal "dead" zone on the level 0 (in the neighbourhood of the point (0,0)) convergence is impossible;

2) in a horizontal zone on the level +5/–5 an error estimate can be found only for higher/lower frequency;

3) in the remaining part of the surface two-frequency convergence is possible and increasing of B widens this area.

On the left of the plots, which correspond to $\omega_{\lg} = \log(\overline{\omega}_d) > 0$, one can see the "Nyquist barrier."

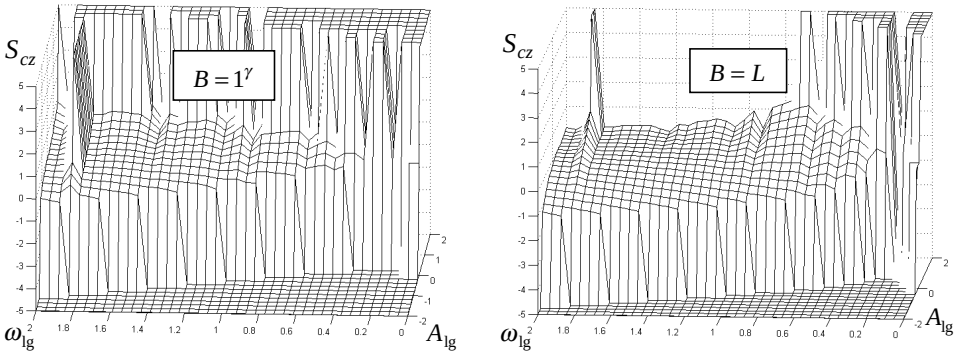

(a) (b)

Fig. 5. Dependence of $S_{cz} = \log(\Psi(\bar{\omega}_d, A_d, B) \Big/ \Psi(\bar{\omega}_d^{-1}, A_d^{-1}, B))$ on $\omega_{\lg} = \log \bar{\omega}_d$ and $A_{\lg} = \log A_d$ for different values of B; $\delta_1 = 0.3$.

3.2. Experiments with EBAFA

In [4] robustness of EBAFA with $Q = 2$ has been demonstrated on an example of a two-component signal, where a waveform of a component with an unlimited $1/f^2$-type spectrum (a rectified sinusoidal signal) was reconstructed (in the experiments this component was either comparable to or 100 times smaller than the other one). In case of the unlimited $1/f$-type spectrum the error signal $e(k)$ appeared to be too big and caused significant distortions of waveforms.

In the experiments considered below we use only such specially generated input signals, which satisfy the Nyquist criterion. The used initial values of the EBAFA's fundamental frequencies were such that the absolute relative frequency errors $|\delta_q| = |(\omega_q - \hat{\omega}_q)/\omega_q|$ were between 10 and 30 per cent.

Figure 6 enables us to compare processing of a four-component signal (fundamental frequencies of its components of different waveforms are $\omega_1 = 0.0535$, $\omega_2 = 0.1308$, $\omega_3 = 0.1319$, and $\omega_4 = 0.3811$, and the levels of these components are comparable) using different frequency error estimators with such values of the parameter K, which appeared to be (nearly) optimal for this signal-processing task.

Comparing the plots in Figs. 6a and b, which correspond to using $D = 1$ and $P = 1$ in Eq. (22) (applying Eq. (16) with $B = P$ and Eq. (21)), where B is determined by Eq. (29), one can see that in case of $P = 1$ the convergence speed of the medium-size frequencies, which are close to each other, is relatively good, but in case of $D = 1$ the frequency convergence process (as a whole) is significantly better.

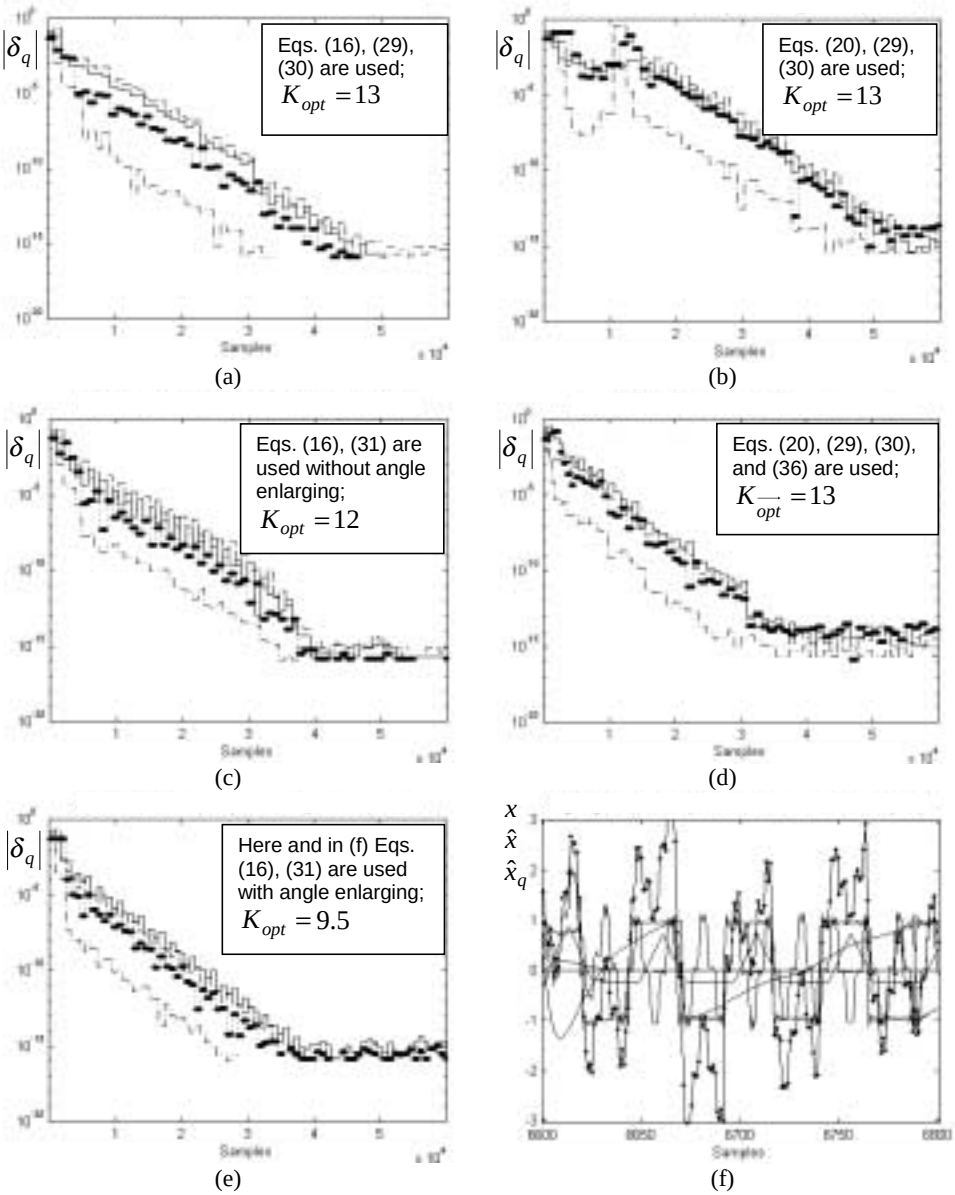

Fig. 6. Processing of a four-component signal in EBAFAs that use different frequency error estimators. In (a) to (e) components' frequency errors $|\delta_q|$ are given for the lowest frequency (dash-dot curve), close ($\delta_\omega \approx 1\%$) medium frequencies (dashed and continuous curves), and for the highest frequency (bold-dotted curve). The plot (f) presents the signals (x is given by dots) in first time-steps when transients do not exceed the input signal's level any more.

Here $P=1$ leads to convergence in the second attempt. However, when EBAFA has to perform such a complicated task as the considered one and its parameter K is far from the optimal value K_{opt} (no matter, which of the considered frequency estimation algorithms is used), one can see not only longer series of such attempts, but also a fully "paralyzed" EBAFA, where all its fundamental frequencies remain (may be, for ever) at erroneous values.

The mentioned undesired processes take place when frequency errors have not been suppressed below certain levels yet, where further convergence is guaranteed (we expect that such levels do exist and further convergence can be proved as in [8] for the BAFA, that is, for EBAFA in the case of $Q=1$). In such situations one can apply two strategies: 1) to avoid steps that lead to great errors, 2) to make (in reasonable time) many steps, among which there would be such ones, which "make things better".

The first strategy, applied in EBAFA in the form of the inequalities (32), gives satisfactory results. In Figs. 6b and e and also in Fig. 7b errors of some fundamental frequencies were not changed in several first convergence steps as the error estimates happened to be unacceptable. A result of one attempt to apply the second strategy is shown in Fig. 6d, where a value of the parameter K for the *k*th frequency error estimation cycle was found as

$$K=\min\{3+k, K_{\text{opt}}\}. \tag{36}$$

This example is presented to emphasize that one has to pay more attention to first frequency adaptation steps in which, in hard conditions, even generally efficient algorithms happen to fail. The considered error estimation algorithms (based on Eq. (22)) are less efficient just in first frequency convergence steps, due to the restrictions (15) and (20).

Better results (Figs. 6e and f) were achieved, when the above described angle enlarging scheme 1 was introduced into the algorithm based on Eq. (22) with $D=1$, improving thus its performance in the first frequency convergence steps too. As in this algorithm the products $B=DP$ are determined using Eq. (31), a parallel experiment without angle enlargement was performed to obtain a basis for comparison (Fig. 6c). Experiments with less complicated signals showed clearly that the angle enlargement increases the convergence speed about 30 per cent.

The best algorithm (based on Eq. (22) with $D=1$ and angle enlargement) was used in EBAFA in the experiments, the results of which are presented in Figs. 7 and 8. In all these experiments $K_{\text{opt}}=2.7$ was used.

The plots in Fig. 7 illustrate processing of an input signal obtained from the one in Fig. 6 after removing one of the components of close to medium frequencies. One can see that different levels of input signal's components do not cause any specific problems: when the greater components have been identified (suppressed) precisely enough, then convergence of the EBAFA's fundamental frequencies onto the frequencies of smaller components is obtained.

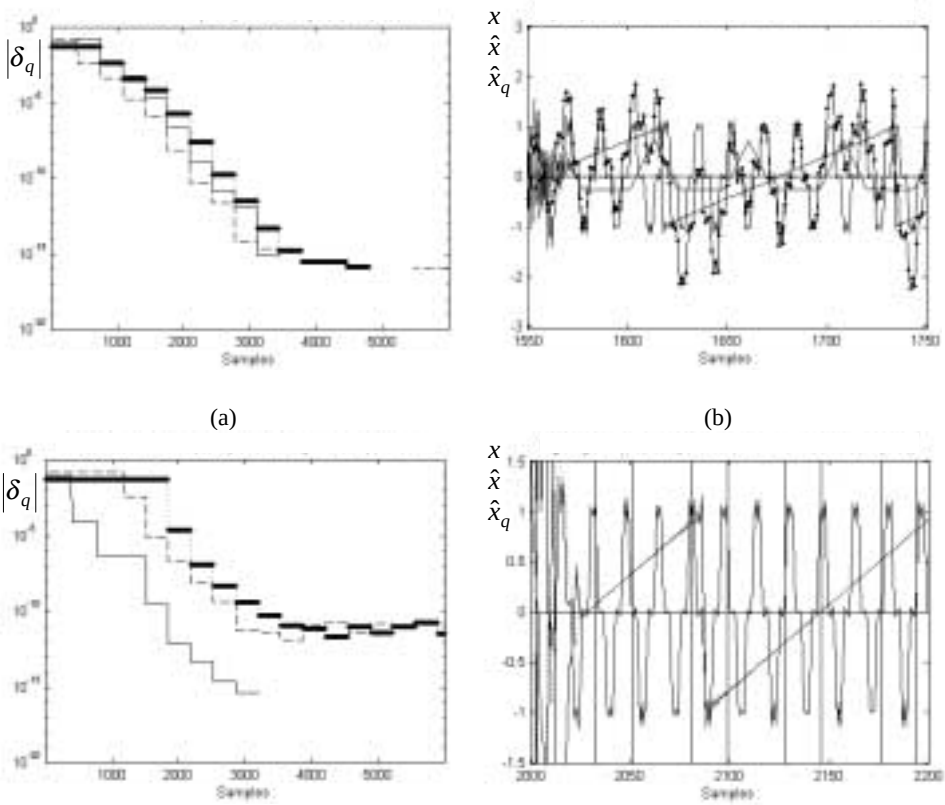

Fig. 7. Processing of a three-component signal in EBAFA of the order $Q = 3$, $K_{\text{opt}} = 2.7$. In the plots (c) and (d) the component of medium frequency (the error of which is given by continuous curve) is 10^6 times greater than in (a) and (b). An acceptable waveform of this component is obtained in time-step 600. In (b) x is given by dots.

Figure 8 demonstrates how EBAFAs of the orders $Q = 4$ and 1 process a single periodic signal, one of the components of the input signal in Fig. 6. With $Q = 4$ the output signals of all the resonator groups, the working bands of which (see Eq. (32)) are empty (that is, do not contain any fundamental harmonics of the input signal), achieve the zero level practically simultaneously. In this experiment we used the same EBAFA and the same initial parameters as in the experiment, illustrated in Figs. 6e and f, with two exceptions: 1) a medium-size fundamental frequency of one resonator group and a corresponding working band were shifted towards the highest fundamental frequency so that the working bands did not overlap, and 2) the used optimal value of K was 2.7 instead of 9.5.

Figure 8a shows that introducing the working bands (the inequalities (32)) enables not only to avoid fatal errors in first frequency convergence steps, but

also to avoid competing of the EBAFA's resonator groups for one and the same input signal's fundamental frequency (Fig. 7b), which can lead to undesired results. The main conclusion is that there is no need to know the exact number of input signal's periodic components, but one has to cover the potential band of input signal's fundamental frequencies with properly chosen (not overlapping) working bands of the EBAFA's resonator groups. Comparison of the plots in Figs. 8a and b shows what is the "cost" of this possibility.

In some experiments, where restrictions were introduced to avoid entering of fundamental frequencies of EBAFA into neighbourhoods of the others and the number of resonator groups was greater than needed, the outputs of the resonators of the redundant groups, which were left "free" (unlocked) in the end of the frequency convergence process, achieved zero value.

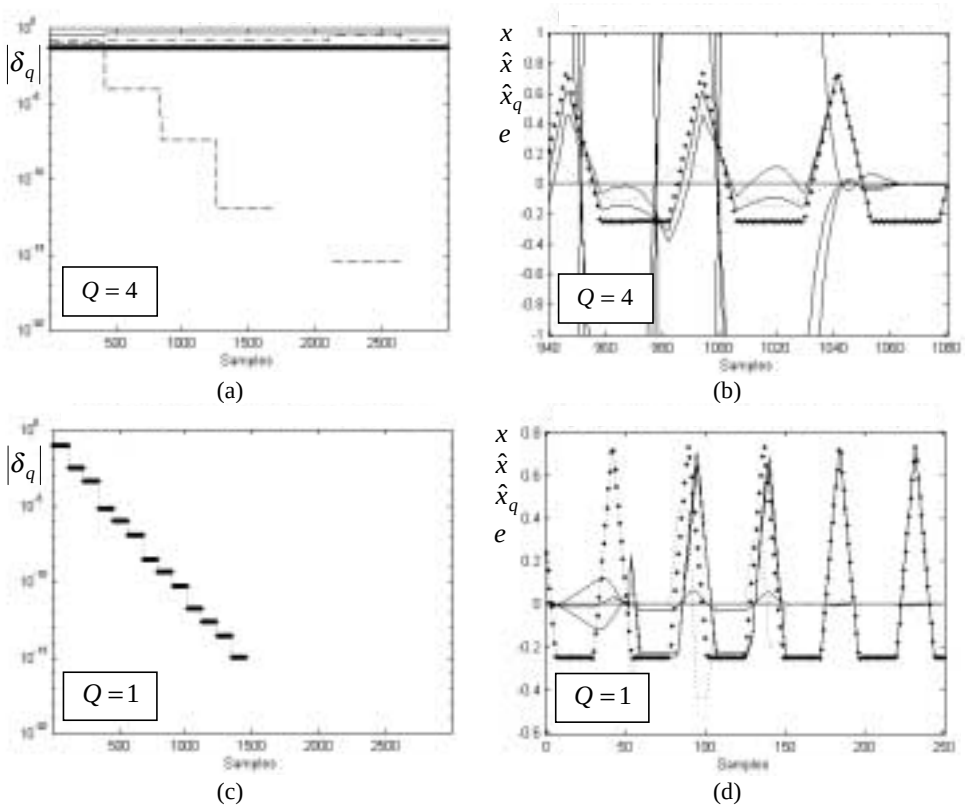

Fig. 8. Processing of a periodic signal in EBAFAs of the orders $Q = 4$ and 1; $K_{\text{opt}} = 2.7$. In the plots (b) and (d) x is given by dots and the error signal e by dotted curve. In the plot (d) a transient of the constant component $\hat{x}_0$ is observable.

4. CONCLUSIONS

The results of investigating frequency adaptation problems in EBAFA, that are presented in this paper and in [4], allow to state the following.

1. The simulation results demonstrate that in certain cases EBAFA is capable to analyse its complicated input signal of the form (1), that is, to reproduce the input signal's periodic components of different frequencies and waveforms, and to find their spectra (complex Fourier coefficients). In these favourable cases, first, the spectrum of the input signal satisfies certain restrictions that are more complicated but rather similar to those formulated for the frequency convergence in BAFA [8]. Second, the fundamental frequencies of the EBAFA's resonator groups $\hat{\omega}_q$ are updated without pitching on certain "bad" sets of values, which lead to too small differences of frequences $\left|m_p\hat{\omega}_p - m_q\hat{\omega}_q\right|$ of some harmonics with numbers m_p and m_q, and to the result that (as it was pointed out in [4]) EBAFA looses its computability. Thus one has to develop an efficient frequency updating algorithm, which guarantees (under certain conditions) avoiding of the mentioned "bad" sets of frequencies $\hat{\omega}_q$. Of course, it is not excluded that the difficulties caused by too close frequencies of higher harmonic resonators can be overcome in some other way.

2. Several new possibilities to improve frequency error estimation in EBAFA and also in BAFA have been proposed and more or less thoroughly analysed and tested. It is obvious that these approaches permit us also to relax restrictions on the input signal. These must be satisfied to achieve (multi-)frequency convergence. Some of them permit enlargement of the measured angle (which is proportional to the error of the frequency error estimate) without increasing the upper limit of its error, to estimate the angle error upper limit, and to make the frequency error estimation algorithm adaptive to the level of the angle error. These means seem to be good enough to modernize EBAFA so that convergence of the fundamental frequencies $\hat{\omega}_q$ to the input signal's frequencies ω_q can be proved under certain preconditions. However, as these preconditions should include (due to the "bad" sets of the fundamental frequencies $\hat{\omega}_q$) a rather low upper limit for the total number of resonators M, this proof is not of serious interest. On the other hand, in case of $Q>1$ the nature of EBAFA (transfer function (9)) as well as that of the input signal (their frequency patterns formed by frequencies of all the harmonics) are such that a change of one fundamental frequency can cause significant changes of the angle errors that appear in the process of estimation of errors of the other (and even unchanged) fundamental frequencies in the next estimation cycle . This important effect of changes of the frequency patterns should be studied more thoroughly with the aim to improve convergence of the frequency vector $\hat{\boldsymbol{\omega}} = [\hat{\omega}_1, \hat{\omega}_2, ..., \hat{\omega}_Q]^T$ to $\boldsymbol{\omega} = [\omega_1, \omega_2, ..., \omega_Q]^T$.

3. As several experiments have shown, EBAFA can be used to analyse a complicated signal even if the exact number of its periodic components of

different frequencies and waveforms is unknown. This important result was achieved due to making a step towards proper treatment of frequency pattern problems and applying, in this particular case, certain restrictions on the EBAFA's fundamental frequencies.

4. The final conclusion is that the above frequency pattern problems must be investigated. The results of this work would enable us to improve the EBAFA and to prove multi-frequency convergence in it under such preconditions, which meet the needs of practice and permit wider application of EBAFA. On the other hand, it would be reasonable to develop application-specific EBAFAs, which meet certain more limited demands.

ACKNOWLEDGEMENT

The author wishes to thank the Estonian Science Foundation for supporting this work under the grants Nos. 2847 and 4862.

REFERENCES

1. Märtens, O., Märtin, H., Min, M., Parve, T., and Ronk, A. Digital post-processing of the bio-impedance signal. In *Proc. X International Conference on Electrical Bio-Impedance (ICEBI'98)*. Barcelona, 1998, 445–448.
2. Widrow, B. and Stearns, S. D. *Adaptive Signal Processing*. Prentice-Hall, Englewood Cliffs, NJ, 1985.
3. Meade, M. L. *Lock-in Amplifiers: Principles and Applications*. Peregrinus, London, 1989.
4. Ronk, A. Separation and analysis of signal's components by means of extended block-adaptive Fourier analyzer. In *Proc. 18th IEEE Instrumentation and Measurement Technology Conference (IMTC/2001).* Budapest, 2001, **2**, 1202–1207.
5. Hostetter, G. H. Recursive discrete Fourier transformation. *IEEE Trans. Acoust., Speech Signal Process.*, 1980, **28**, 184–190.
6. Péceli, G. A common structure for recursive discrete transforms. *IEEE Trans. Circuits Syst.*, 1986, **33**, 1035–1036.
7. Nagy, F. Application of the nonlinear filter and observer theory in adaptive signal processing. In *Proc. IEEE Winter Workshop on Nonlinear Digital Signal Processing*. Tampere, 1993, 6.2-3.1–6.2-3.6.
8. Simon, G. and Péceli, G. Convergence properties of an adaptive Fourier analyzer. *IEEE Trans. Circuits Syst.–II, Analog Digit. Signal Process.*, 1999, **46**, 223–227.
9. Luenberger, D. G. An introduction to observers. *IEEE Trans. Autom. Control*, 1971, **16**, 596–602.
10. Ronk, A. A modified frequency error estimator for the block adaptive Fourier analyzer. In *Proc. Baltic Electronics Conference BEC'2000*. Tallinn, 2000, 103–106.

SAGEDUSADAPTATSIOONIST LAIENDATUD PLOKK-ADAPTIIVSES FOURIER' ANALÜSAATORIS

Ants RONK

On käsitletud sagedusadaptatsiooni võimalusi laiendatud plokk-adaptiivses Fourier' analüsaatoris, milles saab reprodutseerida piiratud sagedusribaga signaali erineva põhisageduse ja kujuga perioodilisi komponente, leides samaaegselt ka nende kompleksse Fourier' rea koefitsiendid (spektrid). On kirjeldatud uusi mooduseid analüsaatori ühe resonaatorirühma põhisageduse vea hindamise algoritmi täiustamiseks. Neid on võrdlevalt analüüsitud ning katsetatud. On tutvustatud ka mitme sageduse adaptatsiooni variante ning uuritud nende rakendatavust MATLABis realiseeritud laiendatud plokk-adaptiivses Fourier' analüsaatoris. Viimasele pole vaja ette anda töödeldava sisendsignaali komponentide täpset arvu.